



## Two metal–organic frameworks (MOFs) based on binuclear and tetranuclear units: Structures, magnetism and photoluminescence

Fang-Hua Zhao, Yun-Xia Che, Ji-Min Zheng\*

Department of Chemistry, Nankai University, Tianjin 300071, PR China

### ARTICLE INFO

#### Article history:

Received 4 July 2011

Received in revised form 23 November 2011

Accepted 24 November 2011

Available online 1 December 2011

#### Keywords:

Mn<sub>2</sub> units

Zn<sub>4</sub> units

Magnetic property

Photoluminescent property

### ABSTRACT

Two new MOFs, [Mn(HBTC)(2-PyBim)(H<sub>2</sub>O)] (**1**) and [Zn<sub>2</sub>(BTC)(OH)(2-PyBim)] (**2**) (H<sub>3</sub>BTC = 1,3,5-benzenetricarboxylic acid, 2-PyBim = 2-(2-pyridyl)benzimidazole), have been hydrothermally synthesized and characterized by single-crystal X-ray diffraction (XRD), infrared spectroscopy (IR), elemental analysis (EA). In **1**, adjacent two Mn(II) ions are connected into binuclear Mn<sub>2</sub> units which are bridged by HBTC<sup>2-</sup> anions to generate a two-dimensional (2D) (4,4) network. In **2**, the Zn(II) ions are connected into tetranuclear Zn<sub>4</sub> units which are bridged by the BTC<sup>3-</sup> anions to generate a 2D (3,6)-connected non-interpenetrating CdI<sub>2</sub>-type network with (4<sup>3</sup>)<sub>2</sub>(4<sup>6</sup> · 6<sup>6</sup> · 8<sup>3</sup>) topology symbol. Both **1** and **2** are extended into 3D supramolecular structure by hydrogen bonds and  $\pi \cdots \pi$  interactions. Magnetic studies of **1** indicate that it exhibits ferromagnetic coupling between the binuclear Mn(II) ions, polymer **2** was found to exhibit photoluminescence at about 437 nm ( $\lambda_{\text{ex}} = 365$  nm).

© 2011 Elsevier B.V. All rights reserved.

### 1. Introduction

In recent years, much research interest has been focused on crystal engineering of metal–organic frameworks (MOFs) or coordination polymers owing to their intriguing unusual topologies and potential applications in many fields such as gas storage, ion exchange, catalysis, magnetism [1,2]. Herein, the rational design and syntheses of MOFs have received considerable interest of many chemists. In construction of the MOFs, the selection of appropriate organic linkers is central to determine the structures of the resulting coordination polymers. And covalent interaction or supramolecular contacts (such as H-bonds and/or  $\pi \cdots \pi$  stacking interactions) [3] are also important factors in preparation of MOFs.

It is well known that the carboxylate ligands play an important role in coordination chemistry owing to their diversity of coordination modes and high structural stability, especially for the multidentate O-donor organic polycarboxylate ligands, such as 1,4-benzenedicarboxylate and 1,3,5-benzenetricarboxylate, have been extensively employed to construct high-dimensional structures [4]. On the other hand, the N-donor ligands such as imidazole, pyridine and their derivatives have also attracted great attention in construction of MOFs [5]. Furthermore, many efforts have been devoted to use of N- and O-donor organic ligands as mixed ligands to bridge metal ions to construct MOFs [6]. As a good N-donor ligand, 2-PyBim (Scheme 1) has larger conjugated  $\pi$ -system than imidazole and 2,2'-bipy, therefore,  $\pi \cdots \pi$  stacking

interactions may play important roles in the construction of its coordination polymers. And the N–H group on imidazole ring of 2-PyBim can be deprotonated or neutral in crystal structures, if it is deprotonated, the two N atoms of imidazole ring can both coordinate to metal centers; if it keeps neutral, the N–H group can act as a proton-donor to form hydrogen bonds, which also may play important roles in the formation of complexes. And only a few examples of transition metal coordination polymers based on 2-PyBim and polycarboxylic acid have been reported [7]. Herein, considering all the aspects above, we report the syntheses and structures of two new MOFs [Mn(HBTC)(2-PyBim)(H<sub>2</sub>O)] (**1**) and [Zn<sub>2</sub>(BTC)(OH)(2-PyBim)] (**2**) based on the H<sub>3</sub>BTC and 2-PyBim ligands. The magnetic, photoluminescent and thermogravimetric properties of **1** and **2** have also been discussed in detail.

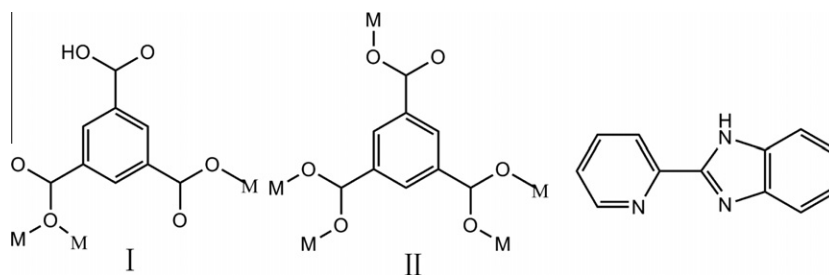
### 2. Experimental

#### 2.1. Materials and measurements

All chemical reagents were purchased commercially and were used as received without further purification. The C, H and N elemental analyses were performed on a Perkin–Elmer 240 C H N elemental analyzer. The FT-IR spectra were recorded from KBr pellets on a Nicolet Magna-IR 560 Infrared spectrometer in the 4000–400 cm<sup>-1</sup> region. Variable-temperature magnetic susceptibility was measured on a Quantum Design MPMS-7 SQUID magnetometer. The photoluminescence measurement was carried out on crystalline samples at room temperature, and the spectra were collected with a Hitachi F-2500FL spectrophotometer. The

\* Corresponding author. Tel./fax: +86 022 23508056.

E-mail address: [jmzheng@nankai.edu.cn](mailto:jmzheng@nankai.edu.cn) (J.-M. Zheng).



**Scheme 1.** Coordination modes of H<sub>3</sub>BTC in **1** and **2**, and the structure of 2-PyBim.

thermogravimetric analyses (TGA) were investigated on a standard TG-DTA analyzer under nitrogen flow at a heating rate of 5 °C/min for all measurements.

## 2.2. Synthesis

### 2.2.1. Synthesis of [Mn(HBTC)(2-PyBim)(H<sub>2</sub>O)] (**1**)

A mixture of H<sub>3</sub>BTC (0.105 g, 0.5 mmol), MnCl<sub>2</sub>·4H<sub>2</sub>O (0.099 g, 0.5 mmol), 2-PyBim (0.098 g, 0.5 mmol) and water (10 mL) was stirred for 30 min. The pH value of the mixture was adjusted to 6.0 with 1 mol L<sup>-1</sup> NaOH solution, and then the resulting mixture was transferred and sealed in a 25 mL Teflon-lined stainless-steel container and heated at 160 °C for 72 h. After slowly cooled to room temperature, the colorless single crystals of **1** were collected. Yield: 55% based on Mn(II). Elemental Anal. Calc. for C<sub>21</sub>H<sub>15</sub>MnN<sub>3</sub>O<sub>7</sub>: C, 52.96; H, 3.17; N, 8.82. Found: C, 52.90; H, 3.11; N, 8.84%. IR (KBr, cm<sup>-1</sup>): 3403 (w), 3078 (w), 1689 (s), 1603 (m), 1561 (s), 1483 (w), 1441 (m), 1392 (w), 1340 (m), 1268 (m), 1102 (w), 1052 (w), 1007 (w), 978 (w), 797 (w), 748 (m), 683 (w), 536 (w).

### 2.2.2. Synthesis of [Zn<sub>2</sub>(BTC)(OH)(2-PyBim)] (**2**)

A mixture of H<sub>3</sub>BTC (0.105 g, 0.5 mmol), Zn(NO<sub>3</sub>)<sub>2</sub>·6H<sub>2</sub>O (0.297 g, 1 mmol), 2-PyBim (0.098 g, 0.5 mmol) and water (10 mL) was stirred for 30 min. The pH value of the mixture was adjusted to 6.0 with 1 mol L<sup>-1</sup> NaOH solution, and then the resulting mixture was transferred and sealed in a 25 mL Teflon-lined stainless-steel container and heated at 160 °C for 72 h. After slowly cooled to room temperature, the colorless single crystals of **2** were collected. Yield: 65% based on Zn(II). Elemental Anal. Calc. for C<sub>21</sub>H<sub>13</sub>N<sub>3</sub>O<sub>7</sub>Zn<sub>2</sub>: C, 45.85; H, 2.38; N, 7.64. Found: C, 45.76; H, 2.40; N, 7.62%. IR (KBr, cm<sup>-1</sup>): 3269 (w), 2859 (w), 2762 (w), 2362 (w), 1614 (s), 1564 (s), 1439 (s), 1371 (s), 1151 (w), 989 (m), 933 (w), 792 (w), 771 (m), 739 (m), 708 (s), 572 (w), 553 (m), 448 (w).

## 2.3. X-ray crystallography

Accurate unit cell parameters of complex **1** and **2** were determined by a least-squares fit of 2θ values, and intensity data was measured on a Rigaku *r*-axis rapid IP area detector with Mo Kα radiation (λ = 0.71073 Å) at 113 K. The intensity was corrected for Lorentz and polarization effects as well as for empirical absorption based on multi-scan technique [8]. The structures were solved by direct method and refined by full-matrix least-squares fitting on F<sup>2</sup> by SHELX-97 [9]. All non-hydrogen atoms were refined anisotropically, the hydrogen atoms bound to carbon atoms were calculated theoretically and those to oxygen and nitrogen atoms were determined by different Fourier maps. Crystal data and structure refinement parameters for **1** and **2** are summarized in Table 1. Selected bond distances and angles are listed in Table S1 and those of the hydrogen bonds are listed in Table S2.

**Table 1**

Crystal data and structure refinement for **1** and **2**.

Complex	<b>1</b>	<b>2</b>
Formula	C <sub>21</sub> H <sub>15</sub> MnN <sub>3</sub> O <sub>7</sub>	C <sub>21</sub> H <sub>13</sub> N <sub>3</sub> O <sub>7</sub> Zn <sub>2</sub>
Formula weight	476.30	550.12
Crystal system	monoclinic	triclinic
Space group	P2 <sub>1</sub> /c	P $\bar{1}$
<i>a</i> (Å)	11.488(1)	10.035(1)
<i>b</i> (Å)	11.014(4)	10.678(2)
<i>c</i> (Å)	16.222(4)	11.189(5)
α (°)	90	79.71(3)
β (°)	107.22(5)	66.48(3)
γ (°)	90	63.96(1)
<i>V</i> (Å <sup>3</sup> )	1960.5(11)	987.7(5)
<i>Z</i>	4	2
<i>D</i> <sub>calc</sub> (g/cm <sup>3</sup> )	1.614	1.850
<i>F</i> (000)	972	552
Reflections collected	18600	9727
( <i>R</i> <sub>int</sub> )	0.1133	0.0364
Independent reflections	4680	4645
Observed reflections [ <i>I</i> > 2σ( <i>I</i> )]	2150	3408
Goodness-of-fit on F <sup>2</sup>	1.003	1.002
<i>R</i> <sub>1</sub> [ <i>I</i> > 2σ( <i>I</i> )] <sup>a</sup>	0.0541	0.0485
<i>wR</i> <sub>2</sub> [ <i>I</i> > 2σ( <i>I</i> )] <sup>b</sup>	0.1236	0.1071

<sup>a</sup>  $R_1 = \sum ||F_o| - |F_c|| / \sum |F_o|$ .

<sup>b</sup>  $wR_2 = \{ \sum [w(F_o^2 - F_c^2)^2] / \sum [w(F_o^2)^2] \}^{1/2}$ .

## 3. Results and discussion

### 3.1. Description of crystal structures

#### 3.1.1. [Mn(HBTC)(2-PyBim)(H<sub>2</sub>O)] (**1**)

Single-crystal X-ray diffraction study reveals that complex **1** crystallizes in the monoclinic P<sub>2</sub><sub>1</sub>/c space group. The asymmetry unit consists of one crystallographically independent Mn(II) ion, one non-completely deprotonated HBTC<sup>2-</sup> anion, one neutral 2-PyBim ligand and one coordinated water. The Mn(II) center exhibits a distorted octahedral coordinated environment, completed by two 2-PyBim nitrogen atoms (Mn–N 2.219(4)–2.336(4) Å), three carboxyl oxygen atoms (Mn–O 2.166(3)–2.180(3) Å) and one water oxygen atom (Mn–O 2.161(3) Å) (Fig. 1a). The non-completely deprotonated HBTC<sup>2-</sup> anion acts as a tridentate bridging spacer linking three Mn(II) atoms with the μ<sub>3</sub>: η<sup>2</sup>, η<sup>1</sup> coordinated mode (Scheme 1, I). Two adjacent Mn(II) centers are bridged by two μ<sub>2</sub>-O<sub>carboxyl</sub> atoms to produce the binuclear Mn<sub>2</sub> units with the Mn···Mn distance of 3.46 Å and Mn–O–Mn angle of 105.15°. The adjacent binuclear Mn<sub>2</sub> units are further connected by HBTC<sup>2-</sup> anions into a rhombic grid with the edge of 9.8 Å, which presents a 2D (4,4) network (Fig. 1b).

In the structure of **1**, neutral 2-PyBim ligands occupy the void of the (4,4) grid in pair and form the intralayer π···π interactions between the two 2-PyBim molecules and between the 2-PyBim and HBTC<sup>2-</sup> ligands with the interplanar separation of 3.626(3), 3.399(3) and 3.806(3) Å, respectively (Table S3). Moreover, the

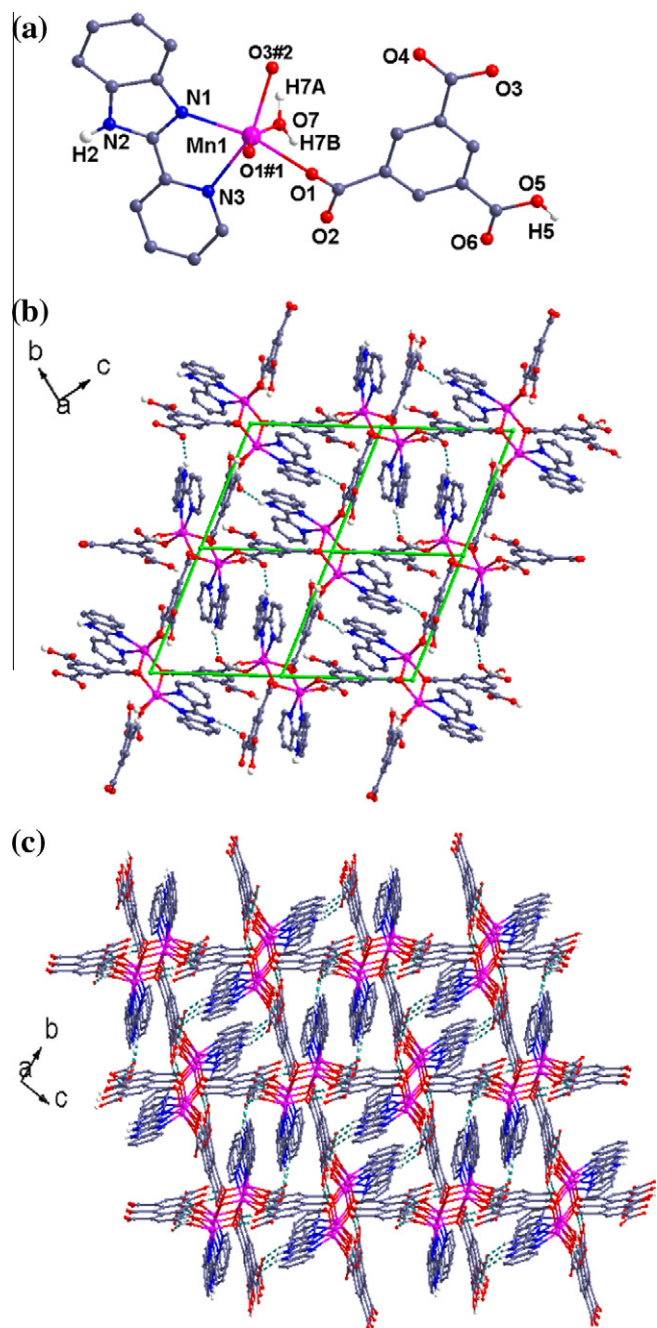


**Fig. 1.** (a) The coordination environment for Mn center in **1**, symmetry code: #1 =  $1 - x, -y, 1 - z$ ; #2 =  $1 - x, 0.5 + y, 1.5 - z$ ; (b) The 2D layer structure of **1** with (4,4) network; (c) View of the 3D supramolecular structure of **1**, the blue dashed lines stand for the hydrogen bonds.

intralayer N2–H2···O4 (2.832(5) Å, 160.2°) hydrogen bond also exists between the 2-PyBim and HBTC<sup>2-</sup> anions. It should be noted that the non-deprotonated carboxyl group of HBTC<sup>2-</sup> anion is uncoordinated but acts as hydrogen-bonds donor and acceptor to form the O5–H5···O2 (2.592(4) Å, 173.7°) and O7–H7B···O6 (2.738(5) Å, 160.4°) hydrogen bonds between adjacent layers. Therefore, the 2D layers of **1** are assembled into a 3D supramolecular structure (Fig. 1c). Similar 2D (4,4) network constructed by binuclear Mn<sub>2</sub> units was previously observed in other complexes: [Mn(HBTC)(BIPY)(H<sub>2</sub>O)] [10a] and [Mn(HBTC)(Pyphen)(H<sub>2</sub>O)]

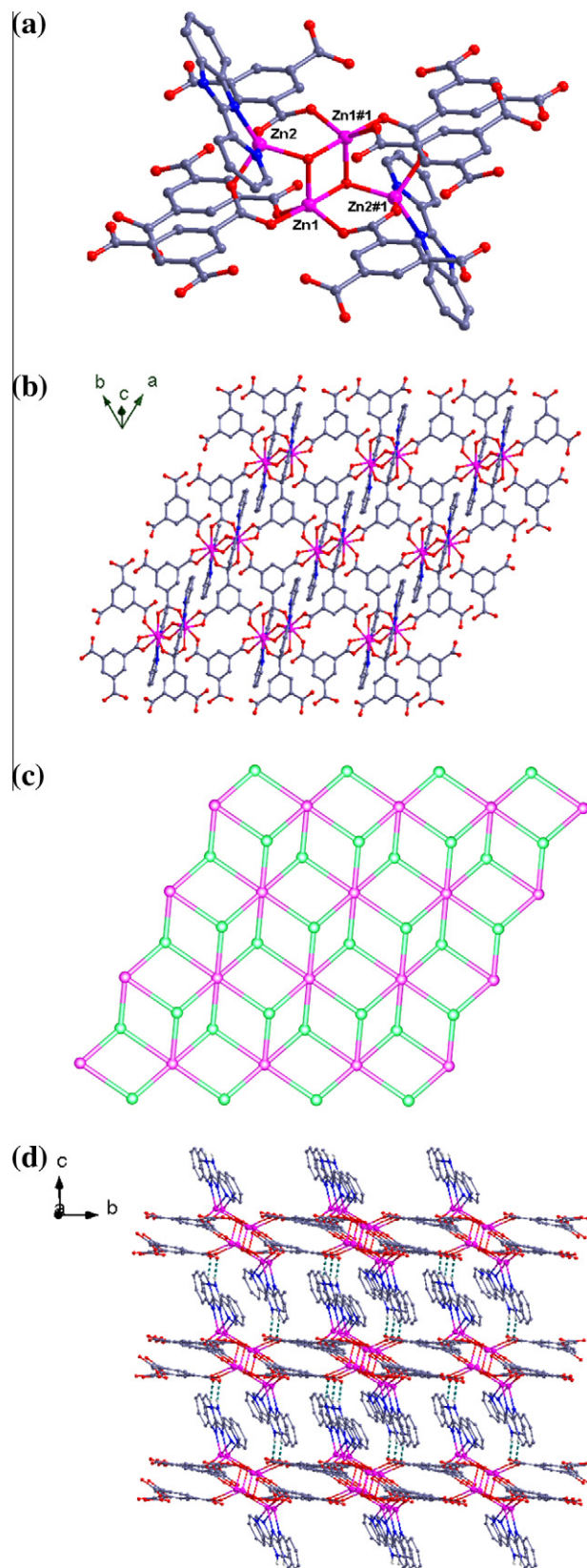


**Fig. 2.** (a) Schematic description of the Zn<sub>4</sub> cluster of **2**, symmetry code: #1 =  $-x, 1 - y, 1 - z$ ; (b) The 2D layer structure of **2**; (c) The topological representation of the 2D layer; (d) The 3D supramolecular structure of **2**, the blue dashed lines stand for the N2–H2···O2 hydrogen bonds.

[10b]. A little difference for **1** is the additional N–H···O hydrogen bonds for the N–H group of imidazole ring in neutral 2-PyBim molecule.

### 3.1.2. [Zn<sub>2</sub>(BTC)(OH)(2-PyBim)] (**2**)

Polymer **2** crystallizes in the triclinic  $P\bar{1}$  space group. The asymmetry unit consists of two Zn(II) ions, one completely deprotonated BTC<sup>3-</sup> anion, one neutral 2-PyBim ligand and one  $\mu_3$ -OH group. Both Zn(II) ions are five coordinated: Zn1 is coordinated by three carboxylic O atoms from three different BTC<sup>3-</sup> anions (Zn–O 1.968(2)–2.072(2) Å) and two O atoms from two  $\mu_3$ -OH groups (Zn–O 2.038(3)–2.111(2) Å) to give the ZnO<sub>5</sub> distorted tetragonal pyramid geometry, while Zn2 is coordinated by two carboxylic O atoms from two different BTC<sup>3-</sup> anions (Zn–O 1.999(3)–2.030(2) Å), one O atom from  $\mu_3$ -OH group (Zn–O 1.952(2) Å) and two N atoms from one neutral 2-PyBim ligand (Zn–N 2.008(4)–2.524(4) Å) to give the ZnO<sub>3</sub>N<sub>2</sub> distorted tetragonal pyramid geometry. Furthermore, two pairs of symmetry-related Zn(II) ions are connected by carboxylic O atoms and two  $\mu_3$ -OH groups to form a tetranuclear Zn<sub>4</sub> unit (Fig. 2a).

In **2**, the completely deprotonated BTC<sup>3-</sup> ligand adopts the  $\mu_5:\eta^2,\eta^2,\eta^1$  coordinated mode (Scheme 1, II), and each of them coordinates to five Zn atoms from three different Zn<sub>4</sub> units. And each Zn<sub>4</sub> unit is bridged by six BTC<sup>3-</sup> anions to form a 2D layer structure with the 2-PyBim ligands on both sides (Fig. 2b). From a topological view, each BTC<sup>3-</sup> ligand can be regarded as a 3-connected node, and the Zn<sub>4</sub> unit is considered as a 6-connected node. As a result, the 2D layer of **2** can be described as a (3,6)-connected non-interpenetrating CdI<sub>2</sub>-type network with (4<sup>3</sup>)<sub>2</sub>(4<sup>6</sup>·6<sup>6</sup>·8<sup>3</sup>) topology (Fig. 2c). The CdI<sub>2</sub>-type network was well known in inorganic compounds [11], but only a few examples were found in the metal–organic coordination frameworks [12]. Polymer **2** is a new example for such network based on 6-connected Zn<sub>4</sub> units.

Similar to **1**, the 2-PyBim ligands maintain neutral and form the  $\pi\cdots\pi$  interactions between adjacent 2-PyBim molecules with the interplanar separation of 3.674(3), 3.580(3) and 3.705(3) Å, respectively (Table S3), no  $\pi\cdots\pi$  interaction were found between the 2-PyBim and BTC<sup>3-</sup> ligands. Finally, the interlayer N2–H2···O2 (2.739(5) Å, 166.0°) hydrogen bonds between 2-PyBim molecules and BTC<sup>3-</sup> ligands connect the layers into a 3D supramolecular structure (Fig. 2d). The framework of **2** is comparable to the previously reported complex of [Zn<sub>2</sub>(OH)(BTC)(Pyphen)] [13]. The (3,6)-connected network of **2** is obviously different from (4,4) net of **1**, which may be attributed to the different coordination modes of the non-completely deprotonated HBTC<sup>2-</sup> and completely deprotonated BTC<sup>3-</sup> in their structures resulting in the binuclear and tetranuclear units, respectively.

### 3.2. Magnetic properties

The variable-temperature magnetic susceptibility measurement of **1** was performed in the temperature range of 2–300 K under a field of 1000 Oe. As shown in Fig. 3a, the  $\chi_{MT}$  value is 4.15 cm<sup>3</sup> mol<sup>-1</sup> K for per Mn(II) ion at room temperature, which is close to the expected value (4.38 cm<sup>3</sup> mol<sup>-1</sup> K) for one magnetism-isolated Mn(II) ion with  $S = 5/2$  and  $g = 2.0$ . The  $\chi_{MT}$  increases continuously to 5.10 cm<sup>3</sup> mol<sup>-1</sup> K with temperature down to 34 K, then increases sharply and finally reaches the maximum value of 7.42 cm<sup>3</sup> mol<sup>-1</sup> K at 2 K, which is characteristic of ferromagnetic behavior. The  $1/\chi_M$  versus  $T$  plot at 30–300 K obeys the Curie–Weiss law [ $\chi_M = C/(T - \theta)$ ] giving Curie constant  $C = 4.06$  cm<sup>3</sup> mol<sup>-1</sup> K and Weiss constant  $\theta = +9.16$  K (Fig. S1). The positive value of  $\theta$  further confirms the ferromagnetic coupling between Mn(II) ions. The temperature-dependent magnetic data for **1** was modeled using a Heisenberg Hamiltonian  $H = -2J S_A \cdot S_B$  which was used

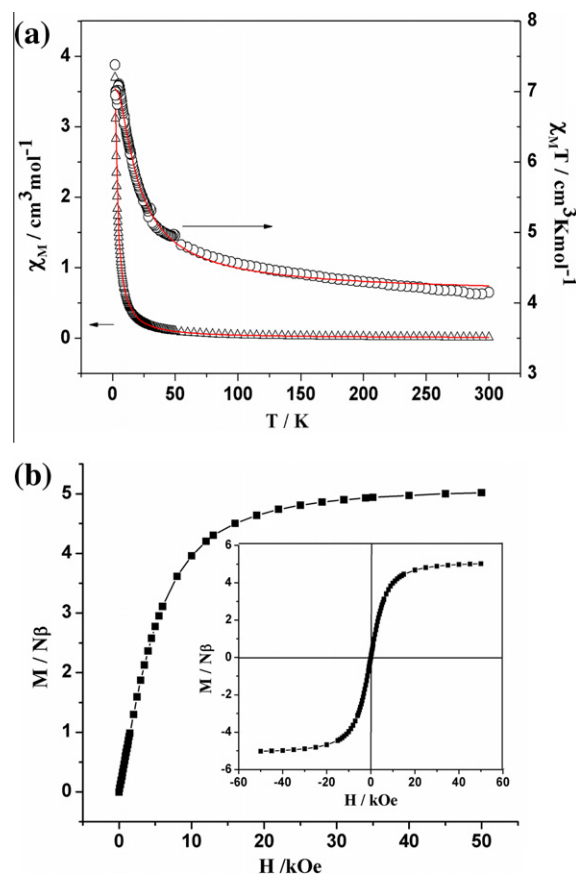


Fig. 3. (a) Temperature dependence of magnetic susceptibility in the form of  $\chi_M$  ( $\Delta$ ) and  $\chi_{MT}$  ( $\circ$ ) vs  $T$  for **1**. The red solid lines are the fits of the data; (b) Magnetization of **1**; Inset: the hysteresis loop for **1** at 2 K.

in study of similar binuclear Mn(II) complex [10a]. The equation below was used to fit the magnetic susceptibility data,

$$\chi_M = (1 - \rho) \times \frac{Ng^2 \beta^2}{kT} \times \frac{e^{2J/kT} + 5e^{6J/kT} + 14e^{12J/kT} + 30e^{20J/kT} + 55e^{30J/kT}}{1 + 3e^{2J/kT} + 5e^{6J/kT} + 7e^{12J/kT} + 9e^{20J/kT} + 11e^{30J/kT}} + \frac{35Ng^2 \beta^2}{12kT} \rho$$

where  $N$  is the Avogadro number,  $g$  is the Zeeman splitting factor,  $\beta$  is the Bohr magneton,  $J$  is the coupling constant,  $k$  is Boltzmann's constant,  $T$  is the absolute temperature,  $\rho$  is the monomeric impurity. The best fitting for the  $\chi_{MT}$  data leads to the parameter values  $J = 1.14$  cm<sup>-1</sup> and  $\rho = 0.3\%$  with reasonable  $g$  factor of 1.94 [14] and  $R = 5.0 \times 10^{-3}$  ( $R = \sum[(\chi_{MT})_{\text{obs}} - (\chi_{MT})_{\text{calc}}]^2 / \sum[(\chi_{MT})_{\text{obs}}]^2$ ); and  $J = 1.22$  cm<sup>-1</sup>,  $\rho = 0.2\%$ ,  $g = 1.94$  and  $R = 2.99 \times 10^{-4}$  ( $R = \sum[(\chi_M)_{\text{obs}} - (\chi_M)_{\text{calc}}]^2 / \sum[(\chi_M)_{\text{obs}}]^2$ ) for the  $\chi_M$  data. The positive  $J$  value indicates ferromagnetic coupling between Mn(II) ions. These results indicate the spin coupling through the HBTC<sup>2-</sup> ligands can be negligible because of the long distance between adjacent Mn<sub>2</sub> units (9.8 Å) bridged by the HBTC<sup>2-</sup> ligands, and the main magnetic exchange pathway is the exchange between neighboring Mn(II) ions via the  $\mu_2$ -O<sub>carboxyl</sub> bridge with the superexchange angle Mn–O<sub>carboxyl</sub>–Mn of 105.15°, which are consistent with the similar example [10a].

Further magnetic characterization of **1** was performed by field dependent magnetization at 2 K under a magnetic field up to 50 kOe. The  $M$  values increase quickly with applied field and finally reaches saturation value of 5.0  $N\beta$  which is excellent close to the

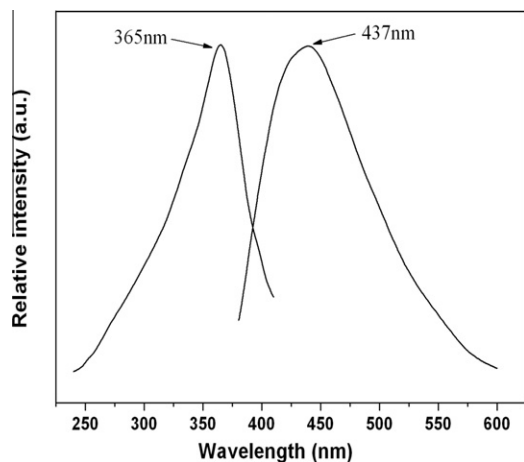


Fig. 4. Excitation (left) and emission (right) spectra in the solid state of **2**.

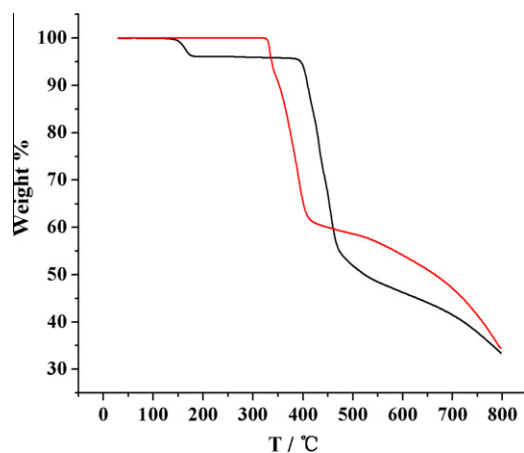


Fig. 5. The TGA diagram of **1** (black line) and **2** (red line). (For interpretation of the references to colour in this figure legend, the reader is referred to the web version of this article.)

expected saturation value of one Mn(II) ion (Fig. 3b), indicating that the ground spin state of the system is the ferromagnetic one [10a]. No magnetic hysteresis loop but a marked s-shaped curve was observed at 2 K (Inset of Fig. 3b), indicating a typical of soft ferromagnet for **1**.

### 3.3. Photoluminescent property

Photoluminescence experiments for Zn-containing polymer **2**, as a typical  $d^{10}$  transition-metal configuration which exhibits photoluminescent property [15,16], were performed at room temperature in the solid state. As shown in Fig. 4, complex **2** displays the emission maxima at 437 nm when excited at 365 nm, which is similar to that observed in other Zn(II) complexes [17]. According to the literature, the free  $H_3BTC$  ligand shows an emission band at 380 nm ( $\lambda_{ex} = 334$  nm) [18], the 2-PyBim ligand shows an emission band at 369 nm [19], thus, the red shift of ca. 57 and 68 nm for **2** relative to the free  $H_3BTC$  and 2-PyBim ligands could be assigned to ligand-to-metal charge-transfer (LMCT) [20].

### 3.4. Thermogravimetric analyses

To estimate the thermostability of complexes **1** and **2**, thermogravimetric analyses (TGA) were carried out in the temperature

range of 30–800 °C under nitrogen with a heating rate of 5 °C/min (Fig. 5). Complex **1** shows a weight loss of 3.85% from 120 to 180 °C, corresponding to the loss of one coordinated water molecule (calcd. 3.78%), and there is no weight loss from 180 to 388 °C; and after that, a rapid weight loss is observed which is attributed to the decomposition of the organic ligands. For complex **2**, no weight loss is observed until it reaches 323 °C, and after that, it begins to chemically decompose. The TGA results show the number of water molecules are consistent with the single-crystal analyses and indicate that complex **2** is more stable than complex **1**.

## 4. Conclusions

In this work, we have synthesized two novel metal–organic complexes based on binuclear and tetranuclear units under hydrothermal condition. The results of this study illustrate that the deprotonation of  $H_3BTC$  ligand plays a central role to determine the structures of the two complexes and the neutral 2-PyBim ligand also plays an important role in the construction of the complexes for the formation of N–H···O hydrogen bonds and  $\pi$ ··· $\pi$  interactions. In addition, the magnetic analyses of **1** display ferromagnetic coupling within the binuclear  $Mn_2$  units, and **2** shows photoluminescent property at room temperature.

## Acknowledgements

This work was supported by the National Natural Science Foundation of China under Project 50872057.

## Appendix A. Supplementary Material

CCDC 807199 and 801999 contain the supplementary crystallographic data for complexes **1** and **2**, respectively. These data can be obtained free of charge from The Cambridge Crystallographic Data Centre via [www.ccdc.cam.ac.uk/data\\_request/cif](http://www.ccdc.cam.ac.uk/data_request/cif). Supplementary data associated with this article can be found, in the online version, at [doi:10.1016/j.ica.2011.11.057](https://doi.org/10.1016/j.ica.2011.11.057).

## References

- [1] (a) O.M. Yaghi, H. Li, C. Davis, D. Richardson, T.L. Groy, *Acc. Chem. Res.* 31 (1998) 474; (b) M.J. Zaworotko, *Angew. Chem., Int. Ed.* 39 (2000) 3052; (c) S.A. Barnett, N.R. Champness, *Coord. Chem. Rev.* 246 (2003) 145; (d) S. Kitagawa, R. Kitaura, S.I. Noro, *Angew. Chem., Int. Ed.* 43 (2004) 2334; (e) B.H. Ye, M.L. Tong, X.M. Chen, *Coord. Chem. Rev.* 249 (2005) 545; (f) J.P. Zhang, X.M. Chen, *J. Am. Chem. Soc.* 131 (2009) 5516; (g) Y.F. Zeng, X. Hu, F.C. Liu, X.H. Bu, *Chem. Soc. Rev.* 38 (2009) 469.
- [2] (a) C. Janiak, *Dalton Trans.* (2003) 2781; (b) C. Janiak, J.K. Vieth, *New J. Chem.* 34 (2010) 2366; (c) S.K. Henninger, H.A. Habib, C. Jania, *J. Am. Chem. Soc.* 131 (2009) 2776; (d) J. Ehrenmann, S.K. Henninger, C. Janiak, *Eur. J. Inorg. Chem.* (2011) 471; (e) U. Mueller, M. Schubert, F. Teich, H. Puetter, K. Schierle-Arndt, J. Pastré, *J. Mater. Chem.* 16 (2006) 626.
- [3] (a) G.R. Desiraju, *Angew. Chem., Int. Ed.* 35 (1995) 2311; (b) C. Janiak, *J. Chem. Soc., Dalton Trans.* (2000) 3885; (c) V. Russel, M.L. Scudder, I.G. Dance, *J. Chem. Soc., Dalton Trans.* (2001) 789; (d) L. Pan, H. Liu, X. Lei, X. Huang, D.H. Olson, N.J. Turro, J. Li, *Angew. Chem., Int. Ed.* 42 (2003) 542; (e) M. Nishio, *CrystEngComm* 6 (2004) 130; (f) W. Wei, M.Y. Wu, Q. Gao, Q.F. Zhang, Y.G. Huang, F.L. Jiang, M.C. Hong, *Inorg. Chem.* 48 (2009) 420.
- [4] (a) S.M.-F. Lo, S.S.-Y. Chui, L.Y. Shek, Z.Y. Lin, X.X. Zhang, G.H. Wen, I.D. Williams, *J. Am. Chem. Soc.* 122 (2000) 6293; (b) A.C. Sudik, A.P. Co te, O.M. Yaghi, *Inorg. Chem.* 44 (2005) 2998; (c) C. Serre, C.M. Draznieks, S. Surblé, N. Audebrand, Y. Filinchuk, G. Férey, *Science* 315 (2007) 1828; (d) W.X. Chen, S.T. Wu, L.S. Long, R.B. Huang, L.S. Zheng, *Cryst. Growth Des.* 7 (2007) 1171; (e) L.G. Qiu, Z.Q. Li, Y. Wu, W. Wang, T. Xu, X. Jiang, *Chem. Commun.* (2008) 3642; (f) J.W. Yoon, Y.K. Seo, Y.K. Hwang, J.S. Chang, H. Leclerc, S. Wuttke, P. Bazin, A.

- Vimont, M. Daturi, E. Bloch, P.L. Llewellyn, C. Serre, P. Horcajada, J.M. Grenche, A.E. Rodrigues, G. Férey, *Angew. Chem., Int. Ed.* 49 (2010) 1.
- [5] (a) Q.D. Liu, W.L. Jia, S. Wang, *Inorg. Chem.* 44 (2005) 1332;;  
(b) Y. Qi, F. Luo, Y.X. Che, J.M. Zheng, *Cryst. Growth Des.* 8 (2008) 606;  
(c) F.J.-B. Dominique, H. Gornitzka, A.S. Saquet, C. Hemmert, *J. Chem. Soc., Dalton Trans.* (2009) 340.
- [6] (a) C.B. Aakerøy, N.R. Champness, C. Janiak, *CrystEngComm* 12 (2010) 22;;  
(b) H.A. Habib, J. Sanchiz, C. Janiak, *Inorg. Chim. Acta.* 362 (2009) 2452;;  
(c) H.A. Habib, A. Hoffmann, H.A. Höpfe, C. Janiak, *Dalton Trans.* (2009) 1742;  
(d) B. Wisser, Y. Lu, C. Janiak, *Z. Anorg. Allg. Chem.* 633 (2007) 1189.
- [7] (a) C.K. Xia, C.Z. Lu, D.Q. Yuan, Q.Z. Zhang, X.Y. Wu, J.J. Zhang, D.M. Wu, *J. Mol. Struct.* 831 (2007) 195;;  
(b) L.J. Zhou, Y.Y. Wang, C.H. Zhou, C.J. Wang, Q.Z. Shi, S.M. Peng, *Cryst. Growth Des.* 7 (2007) 300;;  
(c) W. Li, M.X. Li, J.J. Yang, M. Shao, H.J. Liu, *J. Coord. Chem.* 61 (2008) 2715;  
(d) J. Li, C.C. Ji, L.F. Huang, Y.Z. Li, H.G. Zheng, *Inorg. Chim. Acta.* 371 (2011) 27.
- [8] CrystalClear, version 1.3.5., Rigaku Corp., Woodlands, TX, (1999).
- [9] G.M. Sheldrick, *SHELXL-97: Programs for X-ray Crystal Structure Refinement*; University of Göttingen: Germany, (1997).
- [10] (a) M. John Plater, M.R.St.J. Foreman, E. Coronado, C.J. Gómez-García, A.M.Z. Slawin, *J. Chem. Soc., Dalton Trans.* (1999) 4209;  
(b) G.B. Che, C.B. Liu, B. Liu, Q.W. Wang, Z.L. Xu, *CrystEngComm* 10 (2008) 184.
- [11] (a) C.G. Subhash, A.M. Michael, Y.C. Michael, E.B. William, *J. Am. Chem. Soc.* 113 (1991) 1844;  
(b) M.P. Annika, L.G. Westinand, K.Chem. Mikael, *Chem. Eur. J.* 7 (2001) 3439;;  
(c) D. Thomas, E. Michel, M.L. Yves, A.S.C. Pascale, F. Marcand, B. Patrick, *J. Am. Chem. Soc.* 125 (2003) 3295.
- [12] (a) N. Snejko, C. Cascales, B. Gomez-Lor, E. Gutierrez-Puebla, M. Iglesias, C. Ruiz-Valero, M. Angeles Monge, *Chem. Commun.* (2002) 1366;;  
(b) B. Yan, C.S. Day, A. Lachgar, *Chem. Commun.* (2004) 2390;;  
(c) E.Y. Choi, P.M. Barron, R.W. Novotney, C. Hu, Y.U. Kwon, W. Choe, *CrystEngComm* 10 (2008) 824;;  
(d) Z.B. Han, G.X. Zhang, M.H. Zeng, D.Q. Yuan, Q.R. Fang, J.R. Li, J. Ribas, H.C. Zhou, *Inorg. Chem.* 49 (2010) 769;  
(e) Y.Q. Zheng, X.X. Guo, X.Y. Han, J.H. Xu, *Inorg. Chim. Acta.* 371 (2011) 36.
- [13] Y.Q. Wang, R. Cao, D.F. Sun, W.H. Bi, X. Li, X.J. Li, *J. Mol. Struct.* 657 (2003) 301.
- [14] T. Matsumoto, T. Shiga, M. Noguchi, T. Onuki, G.N. Newton, N. Hoshino, M. Nakano, H. Oshio, *Inorg. Chem.* 49 (2010) 368.
- [15] (a) H.A. Habib, J. Sanchiz, C. Janiak, *Dalton Trans.* 1 (2008) 1734;;  
(b) S. Zang, Y. Su, Y.Z. Li, J. Lin, X. Duan, Q. Meng, S. Gao, *CrystEngComm* 11 (2009) 122;;  
(c) P. Ren, M.L. Liu, J. Zhang, W. Shi, P. Cheng, D.Z. Liao, S.P. Yan, *Dalton Trans.* (2008) 4711;  
(d) W. Liu, Li. Ye, X. Liu, L. Yuan, J. Jiang, C. Yan, *CrystEngComm* 10 (2008) 1395;  
(e) S.L. Zheng, X.M. Chen, *Aust. J. Chem.* 57 (2004) 703.
- [16] M.D. Allendorf, C.A. Bauer, R.K. Bhakta, R.J.T. Houk, *Chem. Soc. Rev.* 38 (2009) 1330.
- [17] (a) X.Q. Liang, X.H. Zhou, C. Chen, H.P. Xiao, Y.Z. Li, J.L. Zuo, X.Z. You, *Cryst. Growth Des.* 9 (2009) 1041;;  
(b) Z.W. Wang, C.C. Ji, J. Li, Z.J. Guo, Y.Z. Li, H.G. Zheng, *Cryst. Growth Des.* 9 (2009) 475.
- [18] J. Yang, Q. Yue, G.D. Li, J.J. Cao, G.H. Li, J.S. Chen, *Inorg. Chem.* 45 (2006) 2857.
- [19] S.M. Yue, H.B. Xu, J.F. Ma, Z.M. Su, Y.H. Kan, H.J. Zhang, *Polyhedron* 25 (2006) 635.
- [20] (a) J.C. Dai, X.T. Wu, Z.Y. Fu, C.P. Cui, S.M. Hu, W.X. Du, L.M. Wu, H.H. Zhang, R.O. Sun, *Inorg. Chem.* 41 (2002) 1391;  
(b) A. Thirumurugan, S. Natarajan, *J. Chem. Soc., Dalton Trans.* (2004) 2923.